V International Conference on Computational Methods in Marine Engineering
MARINE 2013
B. Brinkmann and P. Wriggers (Eds)

ADVANCES IN THE DEVELOPMENT OF A NEW CARTESIAN EXPLICIT SOLVER FOR HYDRODYNAMICS

P. BIGAY[†,*], C. LEROY[†], G. OGER[†], P.-M. GUILCHER[*] AND D. LE TOUZE [†]

[†] L'UNAM Université, Ecole Centrale Nantes, LHEEA lab., ECN / CNRS
1 Rue de la Noë , 44000 Nantes , France

[*] HydrOcean
1 Rue de la Noë CS 32122 44321 Nantes Cedex 3, France
www.hydrocean.fr

Key words: Explicit, Cartesian, Hydrodynamics, Weakly-compressible, Viscosity

Abstract. In order to efficiently address complex problems in hydrodynamics, the advances in the development of a new method are presented here. This new CFD solver aims at obtaining a good compromise in terms of accuracy, computational efficiency, and easy handling of complex geometries. The chosen method is an Explicit Cartesian Finite Volume method for Hydrodynamics (ECFVH) based on a compressible (hyperbolic) solver, with an embedded method for interfaces and geometry handling. The solver's explicit nature is obtained through a weakly-compressible approach chosen to simulate nearly-incompressible flows. The explicit cell-centered resolution allows for an efficient solving of very large simulations together with a straightforward handling of multi-physics. The use of an embedded Cartesian grid ensures accuracy and efficiency, but also implies the need for a specific treatment of complex solid geometries, such as the cut-cell method in the fixed or moving body frame. Robustness of the cut-cell method is ensured by specific procedures to circumvent small cell volume numerical errors. A characteristic flux method for solving the hyperbolic part of the Navier-Stokes equations is used and introduces numerical viscosity. This viscosity is evaluated prior to modeling viscous and turbulent effects. In a first approach presented here viscous effects are computed via a finite difference Laplacian operator introduced as a source term. This solver is validated on 2-D test cases.

1 INTRODUCTION

CFD has become an essential tool for engineers and tends to be more and more affordable in terms of computational costs or available resources. Most solvers in the field of hydrodynamics are implicit under incompressible flow assumption, for which large grid sizes can induce conditioning problems, parallelization difficulties, and nonlinear iterations increase on truly non-stationary problems. Thus, many physical problems such as flows around ships with air entrapment in the bow jet, presence of bubbles in the wake, sea-keeping of boats with complex moving appendages (thrusters...) cannot yet be easily solved. The explicit nature of the proposed method conversely allows for rather straightforward parallelization, robustness and multiphysic simulation handling (multiphase flows, fluid structure). The Cartesian nature of this method allows for a fast and accurate solver.

In this method upwinding is introduced. This, in turn, results in some numerical diffusion.

Prior to modeling physical diffusion and turbulence, a particular care is paid to the assessment of this numerical diffusion, especially according to slope limiters used in the MUSCL scheme of the hyperbolic solution. Then viscous effects are addressed. In the first part of this paper, the compressible core solver is presented. Validation of this solver is achieved through academic test cases and inviscid flow around a cylinder. The second part mainly deals with explicit viscosity modeling. A numerical viscosity study is presented using the Taylor-Green Vortex test case. Finally the explicit viscous solver is validated on classical 2-D test cases such as the Poiseuille flow and the lid-driven cavity flow.

2 ECFVH

2.1 The Navier-Stokes Equations

This method solves the compressible Navier-Stokes equations for viscous compressible flows:

$$\overrightarrow{W_t} + \overrightarrow{\varphi(W)_{x,y,z}} = \overrightarrow{Visc} \tag{1}$$

To close the system and relate pressure and density, we use the Tait isentropic equation of state, thus decoupling the energy equation. This equation is particularly adapted for modeling liquids::

$$P - P_0 = \frac{\rho_0 c_0^2}{\gamma}\left[\left(\frac{\rho}{\rho_0}\right)^{\gamma} - 1\right] \tag{2}$$

with the polytrophic constant γ, a reference pressure P0, the nominal density ρ_0 and the nominal speed of sound c_0.

This equation can be written in the following conservative form:

$$\begin{pmatrix}\rho\\ \rho u\\ \rho v\\ \rho w\end{pmatrix}_t + \begin{pmatrix}\rho u\\ \rho u^2+P\\ \rho uv\\ \rho uw\end{pmatrix}_x + \begin{pmatrix}\rho v\\ \rho vu\\ \rho v^2+P\\ \rho vw\end{pmatrix}_y + \begin{pmatrix}\rho w\\ \rho wu\\ \rho wv\\ \rho w^2+P\end{pmatrix}_z = \overrightarrow{Visc} \tag{3}$$

The viscosity terms in Navier-Stokes equations can be represented as viscous stress tensor components:

$$\overrightarrow{Visc} = \begin{pmatrix} 0 \\ \begin{pmatrix}\tau_{xx}\\ \tau_{xy}\\ \tau_{xz}\end{pmatrix}_x + \begin{pmatrix}\tau_{xy}\\ \tau_{yy}\\ \tau_{yz}\end{pmatrix}_y + \begin{pmatrix}\tau_{xz}\\ \tau_{yz}\\ \tau_{zz}\end{pmatrix}_z \end{pmatrix} \tag{4}$$

It can also be seen as a source term in a Laplacian operator manner as presented in this paper by assuming that compressibility effects in viscosity are negligible due to the weakly-compressible feature of the model.

$$F = \mu \begin{pmatrix} 0 \\ \Delta u \\ \Delta v \\ \Delta w \end{pmatrix} \tag{5}$$

For solving both hyperbolic and elliptic parts, two distinct procedures are setup and described in the next section

2.2 Finite volume characteristic flux scheme

Our solver is based on Finite Volume method, chosen to ensure conservativeness of the method. In this method, the unknowns are located at the center of cells.

To solve the Euler equations a new method originally developed by Ghidaglia et al. [1] in 1996 is used here. This method computes the fluxes needed at each edge by rewriting the equations with the flux Jacobian matrix and using its hyperbolic properties. The solution is then obtained via a projection on the solution in the characteristic base. These fluxes are not expressed in terms of conservative variables as in the Godunov scheme but directly in physical fluxes. For more details, the reader can refer to [2][4][5]. The solution flux is finally expressed as follows:

$$\phi_{Solution} = \left(\frac{F(\overrightarrow{w_L}) + F(\overrightarrow{w_R})}{2} + sign(\overline{\overline{J}}(\overrightarrow{w_{\text{int}}}, \vec{n})) \frac{F(\overrightarrow{w_L}) - F(\overrightarrow{w_R})}{2} \right) . \vec{n} \tag{6}$$

with w_R and w_L the conservative variables vector of left and right cells respectively, w_{int} $\overrightarrow{w_{\text{int}}}$ the value at the interface of the two cells and the Jacobian matrix defined as:

$\overline{\overline{J}} = \frac{\partial \Psi(W,\vec{n})}{\partial W}$. $sign(\overline{\overline{J}}(\overrightarrow{w_{\text{int}}}, \vec{n}))$ is a special matrix constructed with the reduction elements of the Jacobian. This method is an alternative to Roe schemes, HLLE and AUSM+ schemes. This method is general and applicable to any hyperbolic system, easy to implement and efficient in terms of computational costs. The explicit core of the method has been validated on classical test cases such as one and two dimensional shock tubes, backward facing step [2][4][5].

The hyperbolic solving method is based on an upwind method that uses both cell center and face conservative values. To enhance the method and evaluate the latter variables the classical MUSCL scheme [11] is used. Left and right interface values are computed using right and left cell gradients, together with a flux limiting procedure ensuring the Total Variation Diminishing property (TVD) and the non-inversion of the Riemann problem. Flux limiters used have a great deal of importance on the quality and diffusion property of the schemes. Limiters can have a diffusive and/or a dispersive behavior that needs to be evaluated regarding the targeted application. The reconstruction procedure and a few classical limiters are presented in the next page :

$$\begin{cases} u^{D}_{i+\frac{1}{2}} = u_{i+1} - \frac{1}{2}\Theta(\kappa_{i+1})\nabla^{D}u_{i+1} \\ u^{G}_{i+\frac{1}{2}} = u_{i} + \frac{1}{2}\Theta(\kappa_{i})\nabla^{D}u_{i} \\ u^{D}_{i-\frac{1}{2}} = u_{i} - \frac{1}{2}\Theta(\kappa_{i})\nabla^{D}u_{i} \\ u^{G}_{i-\frac{1}{2}} = u_{i-1} + \frac{1}{2}\Theta(\kappa_{i-1})\nabla^{D}u_{i-1} \end{cases} \qquad \kappa_i = \frac{\nabla^{G}u_i}{\nabla^{D}u_i} \tag{7}$$

Minmod (Roe, 1986)	$\Theta(\kappa_i) = Max[0, Min(1, \kappa_i)];$ $\lim_{\kappa_i \to \infty} \Theta(\kappa_i) = 1$
Superbee (Roe, 1986)	$\Theta(\kappa_i) = Max[0, Min(1, 2\kappa_i), Min(2, \kappa_i)];$ $\lim_{\kappa_i \to \infty} \Theta(\kappa_i) = 2$
Van Leer (Van Leer, 1974)	$\Theta(\kappa_i) = (\kappa_i + \lvert\kappa_i\rvert)/(1 + \lvert\kappa_i\rvert);$ $\lim_{\kappa_i \to \infty} \Theta(\kappa_i) = 2$

Table 1. Some of the classical limiters used in the MUSCL scheme.

2.3 Time stepping

Temporal integration stability of the scheme for solving the Euler equations is ensured by respecting the following Courant-Friedrichs-Lewy (CFL) condition based on the area Γ_{int} of the interface between two adjacent cells.

$$dt \leq \min_i \left(\frac{Vol_i}{\Gamma_{\text{int}} \max_k \left| (u_i + c)_k \right|} \right) \tag{8}$$

2.4 Weakly-compressible approach

The specificity of this method resides on the use of a weakly-compressible approach. We indeed use a full compressible model, time step is thus determined via the CFL stability criteria. This criterion leads to very small time steps for near boundary cells, increasing the overall computational costs of the simulations. In order to maximize the time steps and to conserve the physical behavior, the sound speed c_0 is chosen to be about 10 times the maximum value of velocity in the simulations. Simulations are therefore performed at Mach numbers $Ma \approx 0.1$. Under these assumption, it has been shown [6] that the compressible solution can be seen as the superimposition of the incompressible solution and an acoustic solution. Purely compressible effects are negligible ($O(Ma^2)$). Note that such approach is widely used in the SPH community for instance [3].

3 MESHING

Flow simulation around moving complex bodies is a challenging problem, especially when a fixed Cartesian grid is used to discretize the fluid. Local grid modification should be performed on the body surface, without significant increase of the computational cost. Our model is based on the use of cut-cells, together with cell merging procedures to avoid the well-known "small cell" problems, so that reasonable time steps can be preserved [2][4][5]. Cartesian meshing, cut-cell and cell merging techniques therefore allow for an automatic generation of computational meshes (given a surface mesh). An adaptive mesh refinement parallel model will be implemented in the following development steps of the model in order to speed up the computations and to allow massive simulations.

4 INVISCID VALIDATION OF FLOW AROUND A CYLINDER

To validate the hyperbolic solver and the geometry handling, we propose here to study an inviscid flow past a fixed cylinder, with an imposed incident velocity of 1 m/s .This cylinder is located in the center of a 20 meters long infinite tank. As a second step of this study, the pressure solution obtained on this fixed cylinder is then compared to the case of a cylinder moving with an imposed velocity of 1 m/s in a zero velocity flow field. Such conditions are equivalent, so that identical solutions can be expected. In both cases we use potential flow result as an analytical solution. The Van Leer limiter is used here and the results are shown for several grid sizes to show the convergence.

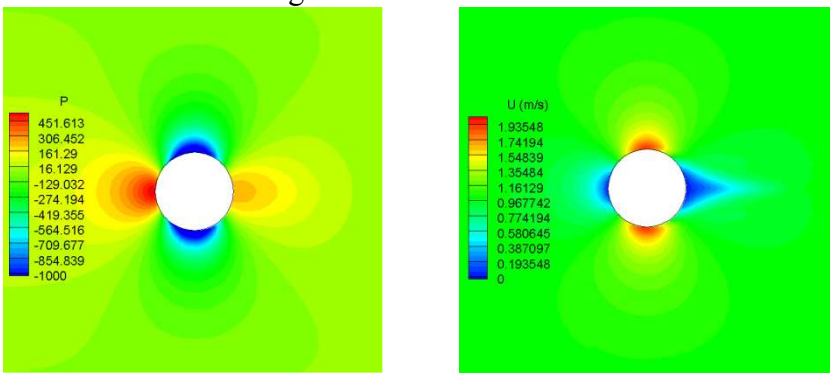

Figure 1. Pressure and velocity fields of the fluid flow around a cylinder.

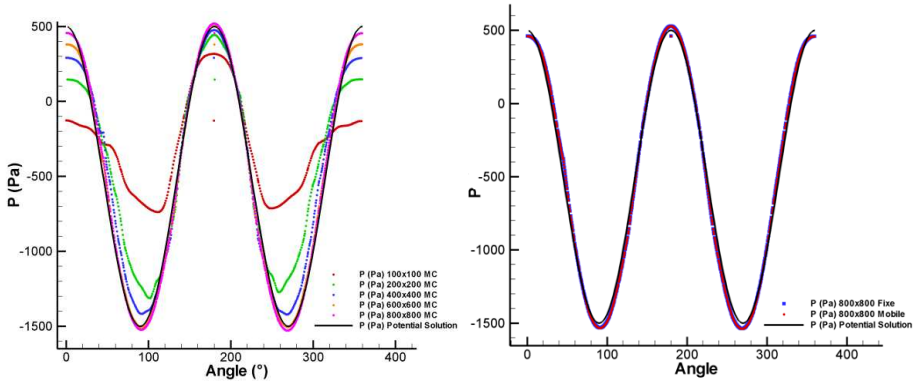

Figure 2. *Local steady pressure around the cylinder for different grid sizes with Van Leer limiter. (left) Local pressure comparison between fixed and moving cylinder(right).*

Previous figures validate the inviscid solver with fixed and moving geometries. Indeed given proper discretizations the pressure profile matches the theoretical potential solution. Fixed and moving solutions match very well thus validating the embedded boundary treatment.

5 VISCOSITY MODELING

5.1 Evaluation of the Numerical Viscosity

Solving the Euler equations requires the use of upwind methods. However these methods are known to be diffusive. In order to properly simulate viscous flows one needs to ensure that numerical viscosity stays negligible compared to physical viscosity. A study is then performed to evaluate this viscosity according to several important factors: discretization, use of MUSCL scheme and flux limiters, and the influence of sound speed.

The use of MUSCL scheme allows to reach second order accuracy for the hyperbolic part. Nevertheless it requires the use of limiters. TVD limiters are very numerous, they are more or less dispersive (overshoots, oscillations in shocks) and diffusive. One of the aims of this study is then to select the limiter with the best trade-off between diffusion and dispersion. The process of selection had a first step (not presented here) where its behavior was studied on 1-D shock tubes. Some limiters (e.g. Superbee) appear to be too dispersive and were not studied in the following test case. Among the tested limiters, only the Minmod and Van Leer limiters are shown in this paper.

To evaluate this numerical viscosity, the Taylor-Green Vortex test case is chosen [9]. This 2-D case consists in four eddies occurring in a square shaped domain of size L. Periodic boundary conditions are imposed at each side of the domain. The initialization is achieved as follows:

$$\begin{cases} u(x,y,t) = U_0 e^{\frac{-8\pi^2 \nu t}{L^2}} \sin\left(2\pi\frac{x}{L}\right)\cos\left(2\pi\frac{y}{L}\right) \\ v(x,y,t) = -U_0 e^{\frac{-8\pi^2 \nu t}{L^2}} \cos\left(2\pi\frac{x}{L}\right)\sin\left(2\pi\frac{y}{L}\right) \\ p(x,y,t) = \frac{\rho U_0^2}{4} e^{\frac{-16\pi^2 \nu t}{L^2}} \left[\cos\left(4\pi\frac{x}{L}\right)+\cos\left(4\pi\frac{y}{L}\right)\right] \\ U_0 = 1m/s, \quad L = 1m, \quad c_0 = 10m/s, \quad \rho_0 = 1000kg/m^3 \end{cases} \tag{9}$$

The initial pressure and velocity fields are presented in the following page.

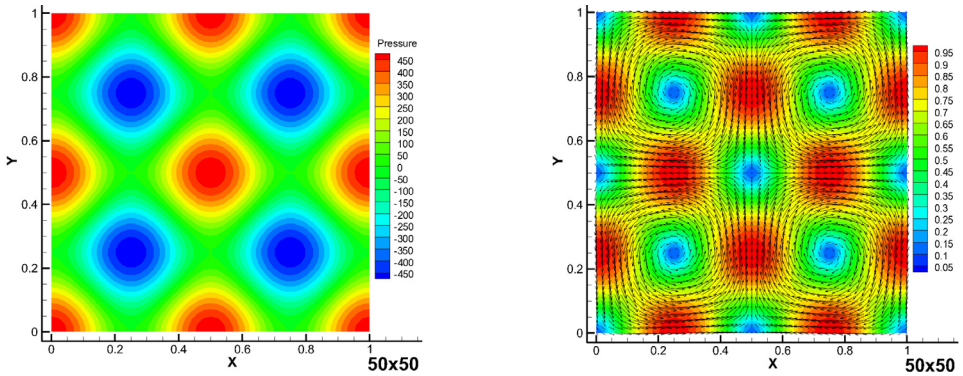

Figure 3. Pressure and Velocity fields of Taylor-Green Vortex test case.

In absence of physical viscosity, the solution is steady. In our case since the method exhibits numerical viscosity, the velocities of eddies decrease. Then by measuring the local velocity decay, it is possible to measure an equivalent numerical kinetic viscosity. Figure 4 shows the velocity decay in time of a point of the flow for different grid sizes.

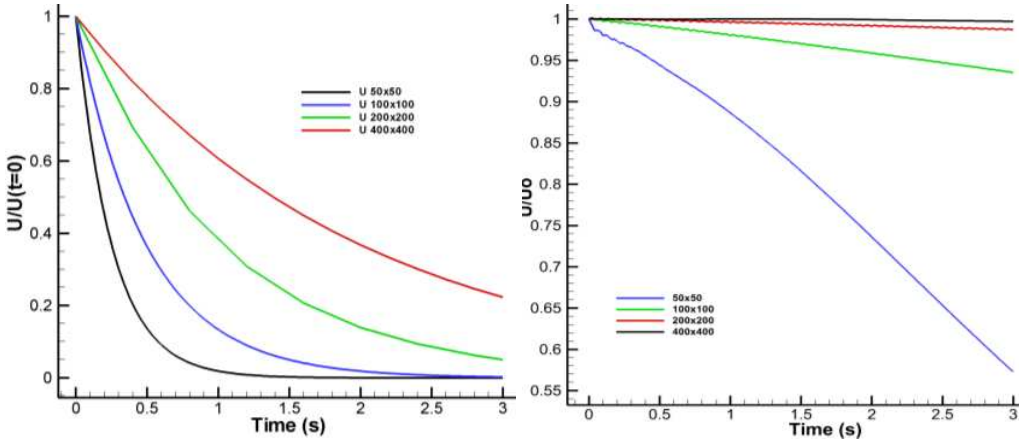

Figure 4. Local velocity of a point for different grid sizes without (left) and with (right) the MUSCL scheme.

As expected the method's upwindind leads to numerical dissipation. Without the MUSCL scheme numerical diffusion is much too important to enable simulating any physical viscosity except for the use of extremely fine grids (in about 3s the eddies are fully dissipated). With the MUSCL scheme, the velocity decay is much less important and will not mask physical viscous effects. To find the better compromise in the MUSCL scheme parametrization, limiters have to be tested in order to achieve the best diffusion/dispersion trade-off. Other than the use of the MUSCL scheme, grid discretization plays an important role: the finer the grids are the less dissipation there is.

The figure below shows the equivalent viscosity without MUSCL, and with MUSCL (Minmod and VanLeer Limiters). As expected, the level of numerical viscosity without MUSCL is too important and would hide all physical viscous effects.

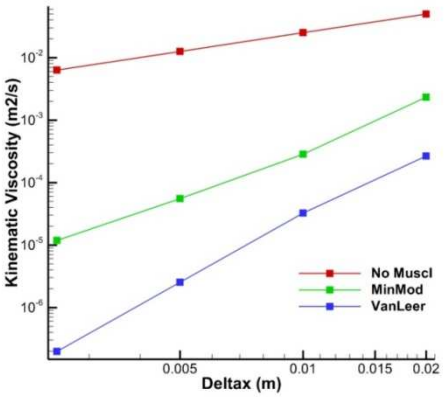

Figure 5. Equivalent kinematic viscosity computed for several discretizations and schemes

Different limiters have been tested, and among them the ones presented in Table 1. The results with the most interesting limiters are presented here. The Minmod limiter is a dissipative-only limiter and Van Leer's one is less diffusive but exhibits a dispersive behavior. According to all the tests performed the latter limiter appears to be the one presenting the best compromise in terms of diffusion and dispersion. A refined grid seems necessary with the Minmod limiter. Results with the Van Leer limiter are better and this limiter is finally adopted in our following simulations. As a conclusion, numerical viscosity will not be an issue for simulating viscous and turbulent flows, especially with turbulent viscosity of an order of magnitude of about 0.001 m^2/s.

5.2 Simulation of physical viscosity

As shown in equations (4) and (5), the elliptic part of Navier Stokes can be computed in two different manners: as a source term or as a viscous flux. In most hydrodynamic CFD codes, viscous terms are computed in an implicit manner. Our choice is to conserve a fully explicit scheme, so that an explicit viscous solver had to be developed.

In this first approach, the source term approach is adopted. To compute viscous effects, second spatial derivatives of velocities are computed at the cell centers. For this Finite Difference schemes, here second order or third order central differences are used (stencil on 3 or 5 points). Central differencing for elliptic schemes is always stable. This solution is robust and quite efficient.

Using this explicit viscous solver requires to respect another stability condition on the time step superimposed to the acoustic one, as:

$$dt \leq \min_i \left(\frac{Vol_i^{\,2}}{\Gamma_{\text{int}}^{\,2} \nu} \right) \tag{10}$$

5.3 Explicit viscous solver validation for low Reynolds number flows

Two different laminar test cases are used in this section to validate this explicit viscous solver: a periodic Poiseuille flow and a lid driven-cavity test cases.

5.3.1 Poiseuille flow

The fluid domain retained for this validation is a square shaped domain of size L = 1 m. The fluid is initialized in the whole domain with a uniform velocity of 1m/s. A longitudinal pressure gradient is imposed as a source term on the flow, while periodic boundary conditions are imposed on the left and right side of the domain to allow the fluid motion in the x direction. No-slip boundary conditions are imposed at top and bottom walls. The theoretical velocity profile expected is parabolic and should write:

$$v(y) = \frac{L^2}{8\eta}\frac{dP}{dx}\left(1 - \frac{4y^2}{L^2}\right) \tag{11}$$

Several simulations for different Reynolds numbers are performed and perfectly match the analytical solution. Here are the results for a 50x50 grid and Re = 1.

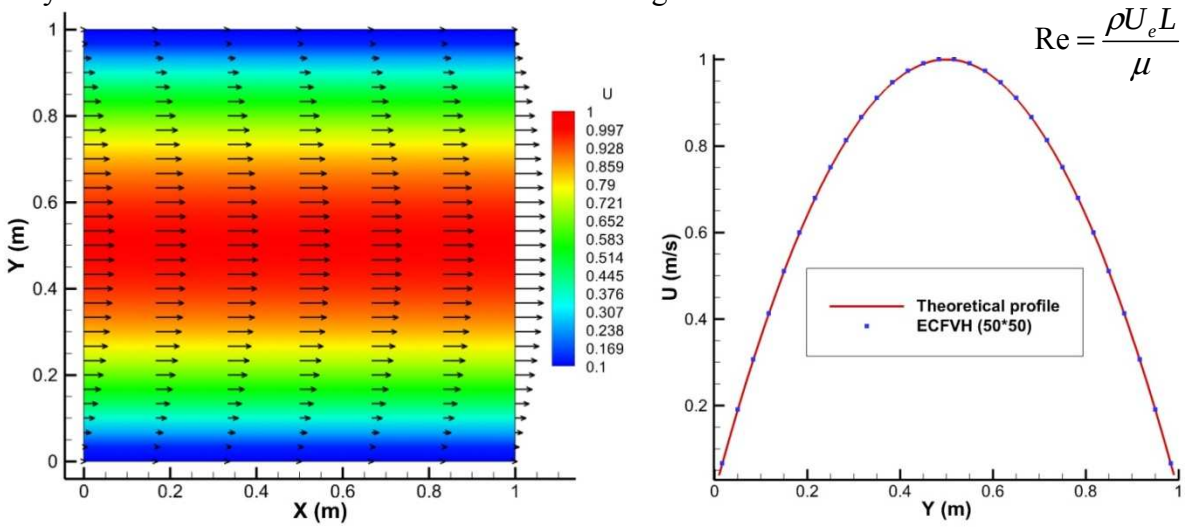

Figure 7. Poiseuille flow velocity field and velocity profile compared to theoretical profile.

5.3.2 Lid-Driven cavity flow

This test case is a classical incompressible test case and has been extensively studied, in particular by Ghia et al. [7]. In this test case, all boundaries are no-slip walls, and the fluid is set into motion by the moving upper wall. Results are available from Re=100 Re=10000. The validation consists in comparing streamlines, velocity profiles at location x=0.5 m and y=0.5 m, and the positions and dimensions of primary and secondary vortexes appearing in the corners.

Simulations have been carried out from Re=100 to Re=3200 for which the flow is still laminar. The velocity of the upper wall is imposed as 1 m/s, and the Reynolds number is varied via the value of the fluid viscosity. All these simulations show very good agreement to

the results available in [7]. In this paper, the results are compared to the reference for *Re*=100 for a grid size of 100x100.

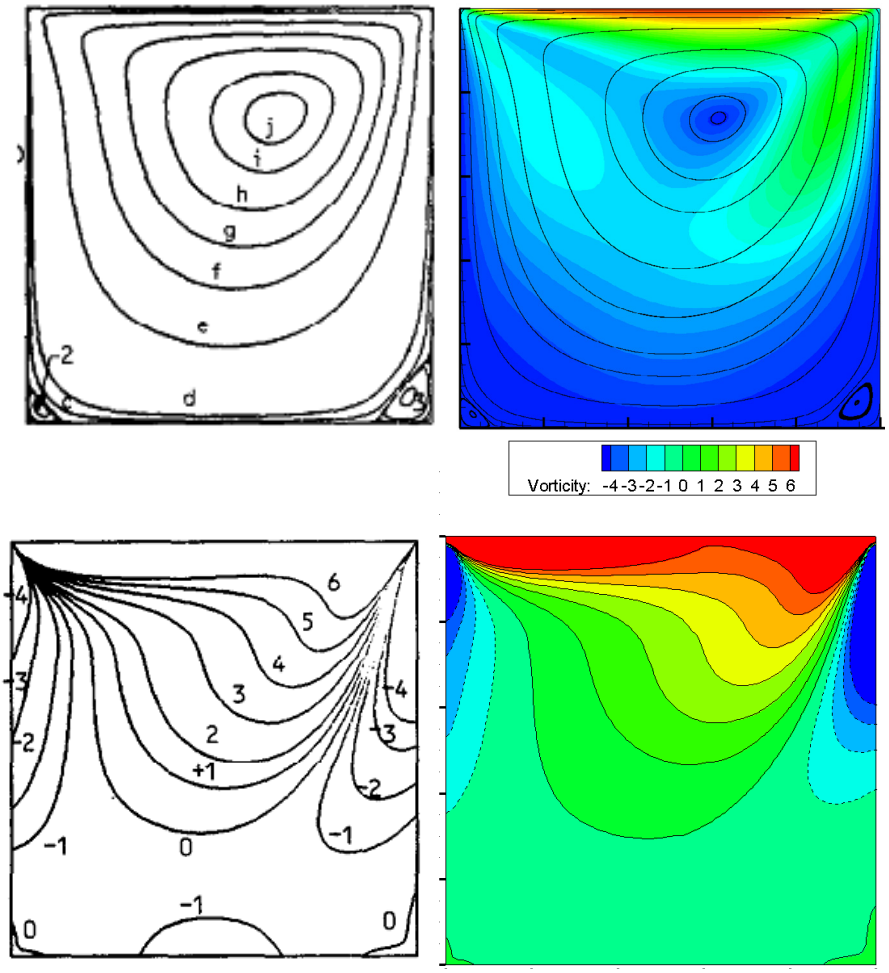

Figure 8. Lid-driven Cavity *Re*=100, Comparison of results with Ghia et al results , Velocity fields and streamlines , Vorticity fields .

The *Re*=100 lid-driven cavity results presented in figure 8 show an excellent agreement with the results from Ghia et al.. The relative errors in positions and dimensions of the vortexes are lower than 2%. Velocity profiles also compare very accurately with the reference.

6 CONCLUSION

A solver based on the Finite Volume method and using upwinded characteristic fluxes has been developed for hydrodynamic flows. This explicit solver relies on a fixed non-conform Cartesian grid into which bodies can freely move thanks to a dedicated cut-cell technique. Simulation of viscous effects has been addressed, namely by studying the influence of numerical viscosity. First validations have been presented on academic test cases, showing very encouraging results. Nevertheless, this method is not straightforward for complex

geometries. Another explicit viscous solver based on viscous fluxes is under development, and methods from [8] and [10] will be investigated. Then higher Reynolds numbers and turbulent simulations will be addressed by means of Large Eddy Simulation (LES). Further developments will also deal with Adaptive Mesh Refinement (AMR) in a parallel framework.

REFERENCES

[1] J.-M. Ghidaglia, A. Kumbaro, G. Le Coq, Une méthode volumes finis à flux caractéristiques pour la résolution numérique des systèmes hyperboliques de lois de conservation, C.R. Acad. Sc. Paris, Vol. 322, pp. 981–988, 1996.

[2] C. Leroy, D. Le Touzé, B. Alessandrini, Development of a cartesian-grid finite-volume characteristic flux model for marine applications, Materials Science and Engineering, Vol. 10, 2010.

[3] D. Le Touzé, G. Oger, B. Alessandrini, Smoothed Particle Hydrodynamics simulation of fast ship flows, Proceedings of the 27th Symposium on Naval Hydrodynamics, Seoul, Korea, 2008.

[4] C. Leroy, P. Bigay, G. Oger, Preliminary developments of a two-fluid Cartesian-Grid Finite-Volume Characteristic Flux model for marine applications. Proceedings of WCCM 2012.

[5] C. Leroy, Développement d'une méthode Volumes Finis à Flux Caractéristiques pour la simulation d'écoulements en hydrodynamique. Phd thesis , 2012.

[6] G. Capdeville, Modélisation numérique d'écoulements compressibles, partie I et II, Polycopié de cours de l'Ecole Centrale de Nantes, 142-149, 2006.

[7] U. Ghia, K.N. Ghia, C.T. Shin, « High-Re Solutions for Incompressible Flow Using the Navier-Stokes Equations and a Multigrid Method », Journal of Computational Physics, vol 48, p. 387-411, 1982..

[8] W.J Coirier, An Adaptively-Refined, Cartesian, Cell-Based Scheme for the Euler and Navier-Stokes Equations, Phd thesis, University of Michigan, 1994.

[9] M. de Leffe, Modélisation d'écoulements visqueux par méthode SPH en vue d'application à l'hydrodynamique navale, Phd thesis, 2011.

[10] M. Berger, M.J. Aftosmis, S. Allmaras, Progress towards a Cartesian cut-cell method for viscous compressible flow, AIAA 2012-1301, 2012.

[11] B.Van Leer, Towards the ultimate conservative difference scheme V. A second order sequel to Godunov's methods, Journal of Computational Physics, Vol. 39, pp. 101-136, 1979.